THE ASTROPHYSICAL JOURNAL, 203:L75–L79, 1976 January 15

CO OBSERVATIONS OF THE BRIGHT-RIMMED CLOUD B35

CHARLES J. LADA AND JOHN H. BLACK
Center for Astrophysics, Harvard College Observatory and Smithsonian Astrophysical Observatory
Received 1975 September 22; revised 1975 October 24

ABSTRACT

Detailed observations of millimeter-wave emission from ^{12}CO and ^{13}CO are made throughout the bright-rimmed molecular cloud B35 and compared with optical photographs. A ridge of enhanced ^{12}CO brightness temperature is observed directly behind and along the bright-rimmed ionization front which forms the western border of the molecular cloud. Measurements of CO column density through the cloud across both the ridge and the ionization front show that the column density peaks near the ridge and, like the CO brightness temperature, steeply decreases across the ionization front. It is shown that modification of the cloud conditions by shock waves can explain our observations and account for the observed CO cooling rates in the cloud. Cloud heating by embedded young stars is also possible, and infrared observations are suggested as a means of distinguishing between the two heating models.

Subject headings: interstellar: molecules

I. INTRODUCTION

Bright rims appear at the interfaces between dense, neutral regions and diffuse nebulae associated with early-type stars. These structures have been recognized since the work of Duncan (1920) and of Struve (1937), and their visible morphology has been described by Thackeray (1950), Osterbrock (1957), and Pottasch (1958, 1959). Bright rims border the neutral material on the side nearest the exciting star and often outline "comet-tail" or "elephant-trunk" patches of obscuring matter which point like dark fingers toward the source of ionization. Bright rims are ionized emission regions and should not be confused with reflection nebulae such as cometary nebulae (Thackeray 1950).

Optical observations indicate that the ion densities in the bright rims are considerably higher than those in the associated diffuse nebulae (Osterbrock 1957; Pottasch 1956, 1958). Observations of molecular lines can now be used to infer the physical conditions within the neutral regions adjacent to the bright rims.

The study of the interaction between hot, ionized regions and cold, neutral condensations is of interest because the attendant shock waves may represent a heat source for molecular clouds and may also induce instabilities which could trigger star formation. We present here detailed CO observations of the dark molecular cloud B35 (Barnard 1927) which is bordered by an extended bright rim. It is significant that the angular extent of this region is large compared with the telescope beamwidth and that the dark cloud and bright rim are located near several T Tauri stars, suggesting a connection with recent star formation.

The bright rim associated with B35 is oriented so that it points toward the O8 III star λ Ori, 4°.5 away. The dark cloud itself lies—in projection—within the giant H II region Sharpless 264, which is about 8° in diameter, has a very low electron density ($n_e = 2$ cm^{-3}), and is excited by λ Ori. In addition to B35, several other dark condensations and bright rims are found at or near the edge of S264, including B30, B36, B223, and B224. A number of T Tauri stars are located near B35 (Herbig and Rao 1972), and the famous peculiar star FU Ori lies inside the cloud near its eastern edge.

II. EQUIPMENT

Our millimeter-wave observations were made during 1974 June using the 5 m millimeter-wave telescope at McDonald Observatory near Fort Davis, Texas.[1] The basic equipment and observing procedure for the CO observations were similar to those described elsewhere (Lada *et al.* 1974*a*). In 1974 June, the single-sideband system temperature was measured by the hot-cold load technique to be about 2000 K for ^{12}CO and about 2400 K for ^{13}CO. All observations reported in this *Letter* were made at source elevations greater than 25°, and a reference position centered on the coordinates of FU Ori ($\alpha = 5^h42^m38^s.2$, $\delta = +9°3'1''.8$; 1950) was monitored as a consistency check for the CO antenna temperatures. In addition, multiplying factors derived by Davis and Vanden Bout (1973) were used to convert the measured ^{12}CO antenna temperatures to Rayleigh-Jeans brightness temperatures (Lada *et al.* 1974*b*).

III. OBSERVATIONS

Observations of the 3 mm line of ^{12}CO were made across B35 in a grid of about 65 points spaced at intervals of 3′, and in a few instances of 1′.5. The Rayleigh-Jeans brightness temperatures determined from these observations are presented in a contour map shown in

[1] The Millimeter Wave Observatory is operated by the Electrical Engineering Research Laboratory, University of Texas at Austin, with support from the National Aeronautics and Space Administration, the National Science Foundation, and McDonald Observatory. The instrumentation used for spectral-line observations with this antenna was developed jointly by the University of Texas, Bell Telephone Laboratories, and the Radio Astronomy Division of the Center for Astrophysics.

Figure 1 (Plate L5) superposed upon a portion of the Palomar Sky Survey red plate of the B35 region. The full-beamwidth grid spacing resulted in some loss of information but allowed time to make a very careful, sensitive map of a large area. Figure 2 (Plate L6) is an enlargement of the red Palomar Sky Survey photograph of B35, reproduced to the same scale and with the same contrast as the photograph in Figure 1. Figure 2 is provided to facilitate comparison of the visible ionization front and obscuring matter with the CO cloud shown in Figure 1.

Comparison of Figures 1 and 2 shows a striking correspondence between the molecular emission and the outline of visible obscuration. The dimensions of the CO cloud within the contour of half peak intensity are $24' \times 30'$ or 3.8 pc × 4.8 pc at the adopted distance of 550 pc. A notable feature of the map is the ridge of enhanced CO emission which resembles very closely the visible bright rim. A steep gradient of CO emission is found west of this ridge across the boundary between the cloud and the rim. The location of this CO ridge strongly suggests that the interaction of the ionization front with the cloud is responsible for—or at least related to—the increase in CO brightness temperature observed in the ridge.

In order to estimate the opacity and column density of CO in B35, we measured ^{13}CO emission at 15 locations within the cloud. The emission lines are relatively narrow, their line widths (uncorrected for instrumental broadening) being 2.29 ± 0.10 km s^{-1} for ^{12}CO and 1.35 ± 0.14 km s^{-1} for ^{13}CO at the peak position (0°.1 north and 0°.2 west of FU Ori). The ratio of Rayleigh-Jeans brightness temperatures is 2.28 ± 0.28, implying a CO column density of $\sim 1.75 \times 10^{18}$ cm^{-2} (Penzias, Jefferts, and Wilson 1971). At the reference position the calculated CO column density is 3.25×10^{17} cm^{-2}. We estimate that the average column density of CO over the area within the 7.5 K contour in Figure 1 is about 5×10^{17} cm^{-2}.

To check the variation in column density across the ionization-front–cloud boundary, we obtained both ^{12}CO and ^{13}CO spectra at four positions along a line of constant declination 0°.1 north of the reference position and intersecting the bright rim. These positions are indicated in Figure 1 (see legend). Figure 3 shows a plot of the calculated CO column density across the molecular-cloud–ionization-front interface 0°.1 north of the reference position. We estimate uncertainties of 20 percent in the calculated column densities, given the usual assumptions of terrestrial isotope ratios, equal excitation temperatures for the two transitions, and saturation of the $J = 1 \rightarrow 0$ line of ^{12}CO.

Figure 3 shows that the calculated CO column density is enhanced by at least a factor of 3 in the high-temperature ridge compared with the rest of the cloud ahead of the ionization front. Across the cloud-front boundary, a dramatic decrease in column density is recorded. One beamwidth west of the peak in Figure 3, the calculated column density drops by a factor of more than 20. Although our grid is incomplete in this area, the observations clearly show enhancements of molecular column density ahead of the ionization front and of molecule destruction rate across the ionization front.

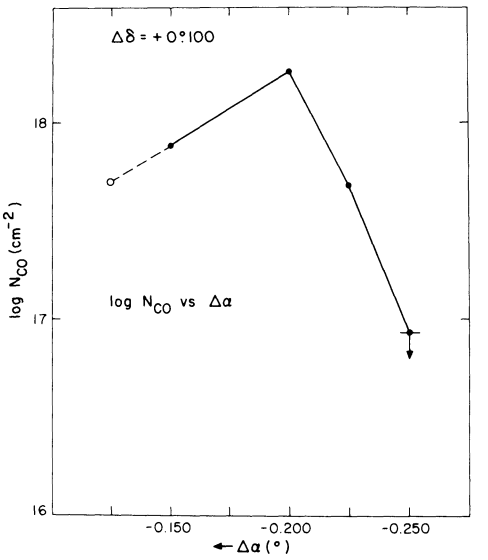

FIG. 3.—Plot of CO column density as a function of α_{1950} at a declination of +0°.1 north of the reference position (FU Ori). This graph shows the variation of CO column density across both the high temperature ridge and the ionization front seen in Figure 1. The filled points represent measurements taken at the positions indicated in Figure 1. The open data point represents the estimated average CO column density outside the high temperature ridge (see text).

The high intensity of ^{13}CO relative to the main species indicates that the ^{12}CO line has a very large optical depth; therefore, the brightness temperature of ^{12}CO is probably very near the actual kinetic temperature of the cloud. Recent detection of the $3_2 \rightarrow 2_1$ transition of SO at 99 GHz toward the high-temperature ridge (Gottlieb *et al.* 1975) implies densities of H_2 of about 10^4 cm^{-3}, so the lower rotational levels of CO are likely to be thermalized there. Consequently, kinetic temperatures can be obtained by correcting the observed ^{12}CO spectra for the Rayleigh-Jeans approximation, and by assuming a background temperature of 2.7 K behind B35. The maximum kinetic temperature in the cloud is approximately 20 K. The increased ^{12}CO brightness temperature thus reflects an increase in the kinetic temperature along and directly ahead of the ionization front.

Figure 4 is a map of the integrated ^{12}CO line intensity. Three peaks of integrated line intensity are found along and at the edge of the cloud-front interface. These peaks are located within the ridge of peak CO emission in Figure 1. As with the brightness temperature map in Figure 1, the contours in Figure 4 show a very sharp downward gradient in the westward direction across the cloud-front boundary. Figures 1, 3, and 4 suggest that the physical conditions within the cloud have been affected by the penetration of the ionization front which is visible as the bright rim around B35.

IV. DISCUSSION

a) Shock Wave Models

An attractive explanation of the enhancements of temperature and CO column density along the western boundary of B35 is provided by the passage of a shock

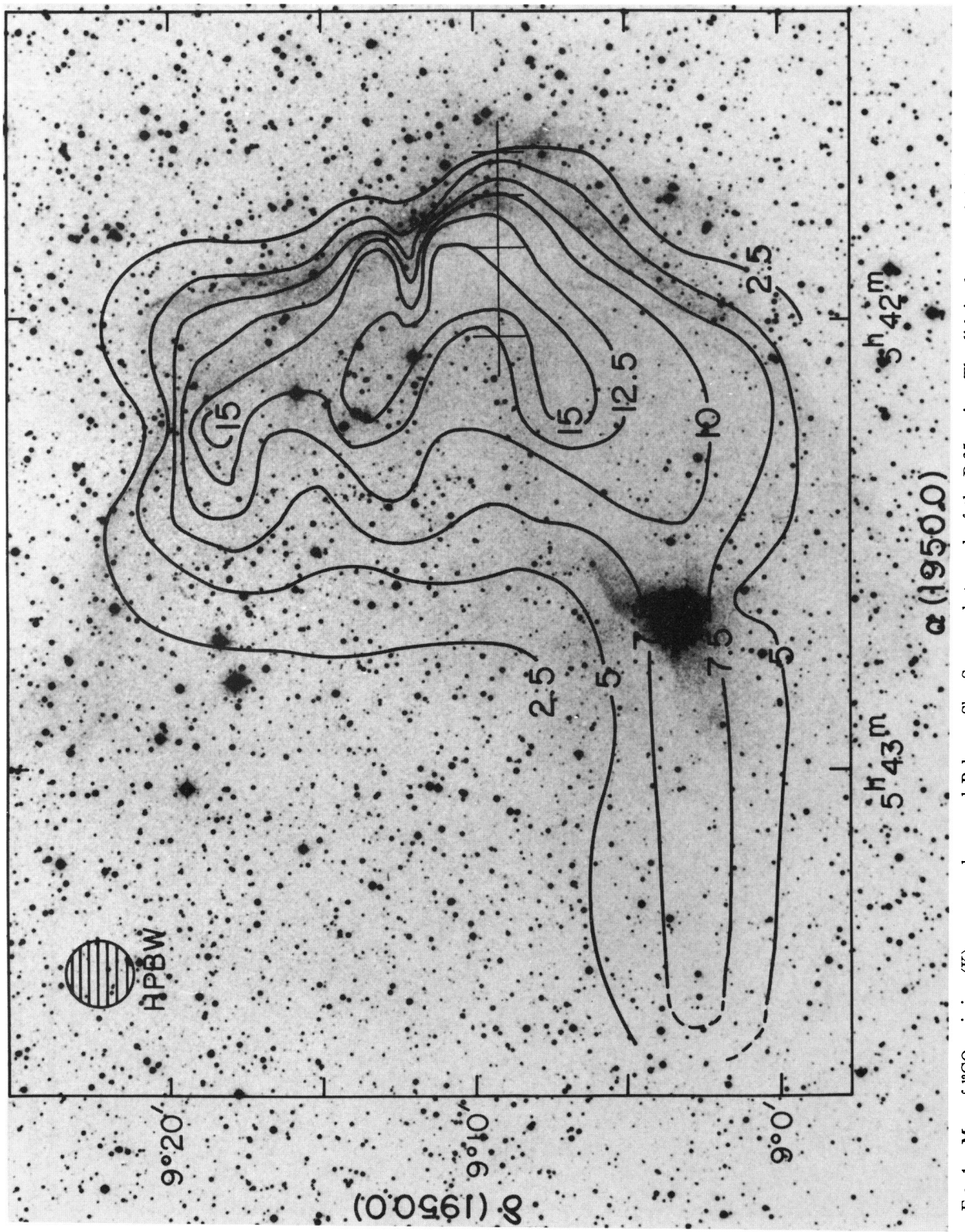

FIG. 1.—Map of ^{12}CO emission (K) superposed on a red Palomar Sky Survey photograph of the B 35 region. The disk in the upper left hand corner represents the size of the telescope's beamwidth (HPBW). The positions of CO column density measurements are indicated by the horizontal line with vertical marks. See Figure 3.

LADA and BLACK (*see* page L76)

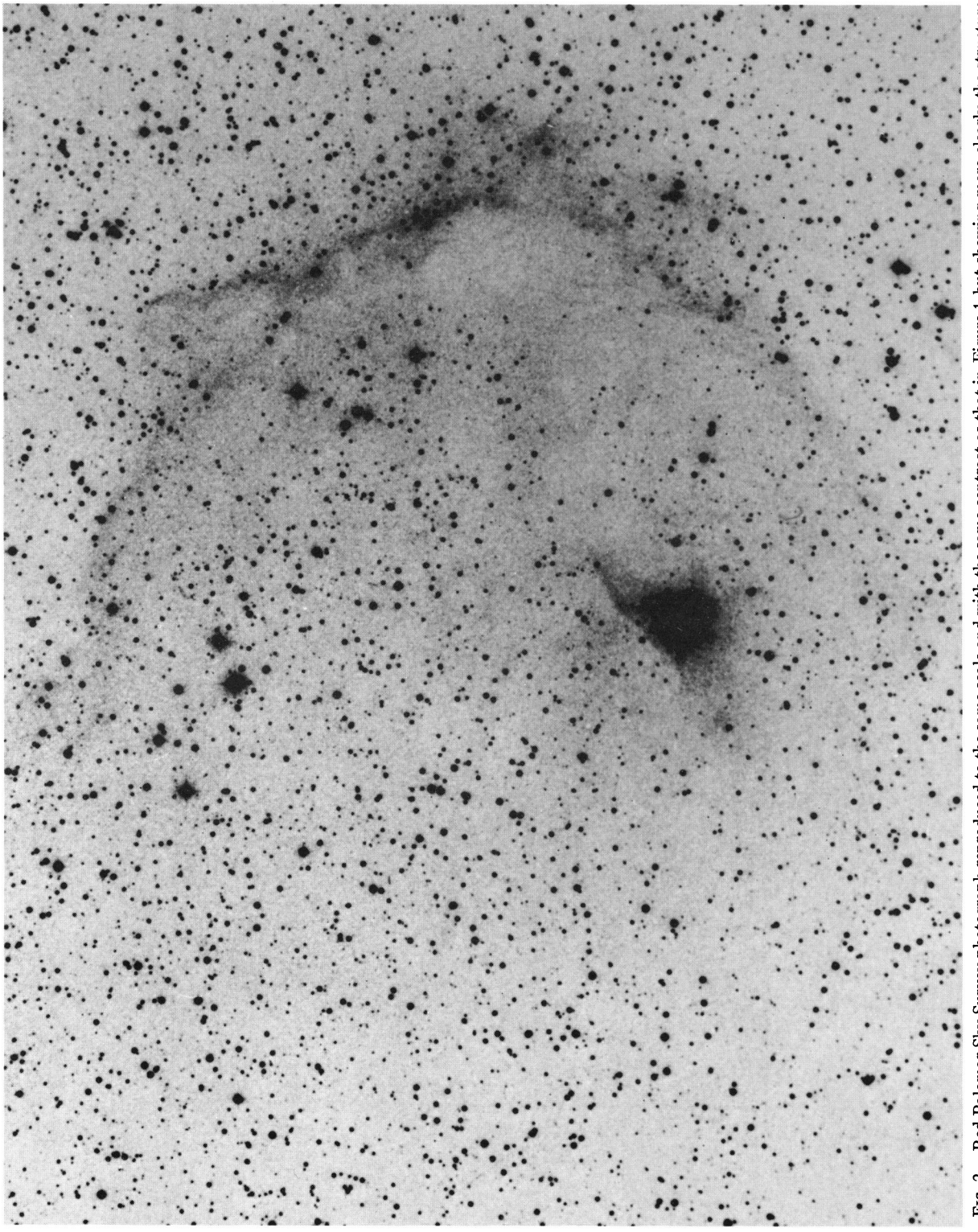

FIG. 2.—Red Palomar Sky Survey photograph reproduced to the same scale and with the same contrast as that in Figure 1 but showing more clearly the structure in the bright rim.

LADA and BLACK (*see* page L76)

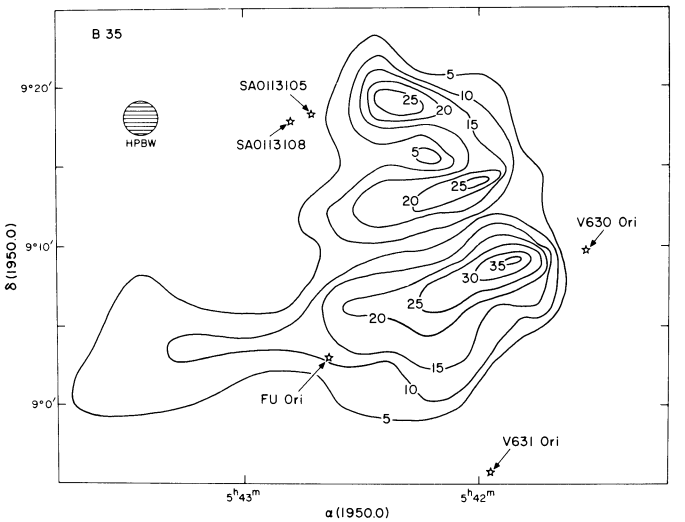

FIG. 4.—Plot of integrated ^{12}CO line intensity (i.e., $T_b\Delta V$) toward B35. Units are K km s^{-1}. The positions of FU Ori, and two T Tauri stars, V630 Ori and V631 Ori, are indicated.

wave preceding the ionization front. Shocks are generally expected to accompany ionization discontinuities in the interstellar medium. In the case of interest here, the effect of the shock will be the heating and compression of the gas immediately behind the shock front and ahead of the ionization front. It is of interest to compare the physical conditions inferred from observation in B35 with a simple model. Approximate treatments (Kahn 1954; Pottasch 1958; Kaplan 1966) are adequate for a preliminary description of the temperature and density structure and for a rough audit of the energy budget in the shocked gas.

Consider an ionization front separating a fully ionized region of proton density n_2 from a neutral cloud having a density of atomic hydrogen, n_1. If U_1 and U_2 are the gas velocities in the neutral and ionized regions, respectively, relative to the front, then the condition of conservation of matter crossing the front may be written

$$n_1U_1 = n_2U_2 = J\,, \qquad (1)$$

where J is the ionizing flux normally incident upon the front in photons cm^{-2} s^{-1}. It is assumed that the flux of photons capable of dissociating H_2 is sufficiently high in the immediate vicinity of the front that the neutral matter will be atomic insofar as the discontinuity conditions are concerned.

Following Pottasch (1958), we write the mean energy input into the gas per ionizing photon as $\epsilon = \frac{1}{2}m_pQ^2$, where m_p is the proton mass and, for a 35,000 K blackbody (taken to represent λ Ori), $Q = 2.9 \times 10^6$ cm s^{-1}. For the case of a one-dimensional, D-critical front (Kahn 1954; Pottasch 1958), the approximate solution of the conservation of matter, momentum, and energy equations across the front results in the expressions

$$n_1 = \frac{4QJ}{3c_1^2}\,, \qquad n_2 = \frac{2J}{Q}\,, \qquad (2)$$

where c_1 is the sonic velocity in the neutral gas. In this simple picture, the density n_2 depends only upon the luminosity in ionizing photons of the star and its distance from the front. The distance of B35 and its bright rim from λ Ori is assumed to be the visible radius of the H II region at the position angle through the center of the bright rim. This radius is 44 pc if λ Ori is 550 pc away. We take $J = 2.5 \times 10^7$ photons cm^{-2} s^{-1} at the front with the result that $n_2 = 17$ cm^{-3}. In atomic hydrogen at $T_1 = 100$ K, $c_1 = 1.2 \times 10^5$ cm s^{-1}; hence, $n_1 = 6700$ cm^{-3}. Although the kinetic temperature of 100 K is assumed rather than measured, it is not likely to be seriously in error given the nature of the dominant coolant (C^+ fine-structure transitions) in a neutral atomic region.

In B35 we observe a molecular cloud directly ahead of the H I region. The observations of CO suggest a kinetic temperature of 20 K in the molecular cloud. If the molecular cloud is in pressure equilibrium with the H I region, the molecular hydrogen density is about 3×10^4 cm^{-3}, a value consistent with the detection of SO in the molecular ridge and with the assumption that the lower rotational levels of CO are thermalized. The rate of cooling due to CO in a normal H_2 cloud at the density and temperature inferred above is roughly 3×10^{-23} ergs cm^{-3} s^{-1} (De Jong, Chu, and Dalgarno 1975). It is of interest to verify whether the energy deposited into B35 by a shock can balance the inferred rate of cooling.

The energy radiated instantaneously by a luminous shock is

$$E = \tfrac{1}{2}\rho_0V_s^3/\Delta x\,, \qquad (3)$$

where ρ_0 is the mass density of the undisturbed gas ahead of the shock and V_s is the velocity of the shock with respect to this gas. The length Δx is a characteristic cooling scale for the shock-heated gas. Illustrative results may be obtained using the similarity solutions of Kaplan (1966) for the case of an isothermal, one-dimensional shock–ionization-front system. In Kaplan's treatment

$$V_s = 2(\rho_2RT_2/\rho_0\mu_2)^{1/2}\,, \qquad (4)$$

where R is the gas constant, T_2 is the temperature at the ionization front (about 10^4 K), and μ_2 is the molecular weight of the gas in the H II region. The separation of the shock and ionization fronts relative to the Stromgren radius is given by

$$\Delta r/r = T_1/(4T_2)\,[\rho_0/\rho_2 - (\rho_0/2\rho_2)^{1/2}]\,. \quad (5)$$

In the case of B35, we identify the ionization front with the bright rim and the shock front with the eastern edge of the ridge of enhanced CO emission, so that $\Delta r/r = 0.023$. With this value and the adopted temperatures, the ratio of densities ρ_0/ρ_2 may be determined from equation (5) which in turn provides an estimate of the shock velocity (4). The results of this simple analysis are that $\rho_2 = 17\ m_{\rm H}$ (eq. [2]), $\rho_0 = 200\ m_{\rm H}$, and $V_s = 7.5$ km s^{-1}, so that equation (3) gives $E = 2 \times 10^{-23}$ ergs cm^{-3} s^{-1}, with $\Delta x \approx \Delta r$.

Immediately behind the shock, temperatures as high as several thousand kelvins may occur. The cooling time appropriate for a temperature decrease from 3000 K to 30 K is of the order of $t_{\rm cool} = 1000$ years, while 10^5 years may be required for further cooling down to an equilibrium temperature of 10 K, typical of a molecular cloud (cf. Spitzer 1968). Although the efficiency of the high-temperature coolants such as H_2 is roughly 100 times that of the low-temperature coolants such as CO (Aannestad 1973), the distance $V_s t_{\rm cool}$ over which the low-temperature coolants dominate is so much larger than the hot, immediate postshock region that the radiant energy actually measured as CO photons accounts for as much as half the total energy supplied by passage of the shock. Therefore, to an order of magnitude, the CO flux may be adequately accounted for by the presence of a shock wave in B35.

b) *Alternative Interpretations*

In almost all other molecular clouds (e.g., Orion, M17, L1630, M8, and NGC 1333) CO emission peaks are strongly correlated with infrared point sources which probably represent internal heat sources (Goldreich and Kwan 1974). Similarly, the ridge of enhanced emission in B35 might result from heating by embedded stars or protostars rather than from passage of a shock. Loren, Peters, and Vanden Bout (1975) have, in fact, ascribed CO emission in another bright-rimmed cloud to internal heating. The discovery of infrared sources embedded in B35 would be very interesting, particularly in a region where shock activity is to be expected. A shock wave could already have passed through much of the cloud, compressing the gas and triggering star formation in its wake, with the protostars formed at that time now dominating the heating in the ridge. We note that the three peaks of integrated line intensity in Figure 4 are separated by approximately the gravitational instability length for a uniform disk (Spitzer 1968), and it would be interesting to search for infrared sources at these positions.

Four known T Tauri stars are located just west of the bright rim (Herbig and Rao 1972). Two of these, V630 Ori and V631 Ori, have projected distances of 0.5 and 0.7 pc, respectively, from the rim. These stars could conceivably have formed from the compressed gas ahead of the ionization front to then be revealed by the passage of the front and the subsequent dissipation of their embryonic envelopes about 5×10^5 years ago.

V. CONCLUSION

Carbon monoxide observations of the dark cloud B35 show an interesting ridge of enhanced emission near a prominent bright rim. A simple analysis has shown that the observations are consistent with heating and compression by a shock wave preceding the ionization front (bright rim). However, heating of the cloud by embedded stars formed in the shock-compressed gas ahead of the ionization front could also be responsible for the observed CO emission ridge. We suggest searches for infrared point sources to help distinguish between shock and internal source heating models for B35.

We suggest that ionization fronts and shock waves may play a very important role in determining the physical conditions in bright-rimmed molecular clouds as well as in the processes of star formation and cloud dissipation. Since many other prolific star-forming regions are very closely associated with ionization fronts (Elliot and Meaburn 1974; Lada 1975; Lada *et al.* 1976), a clearer understanding of the effects of shock and ionization fronts on the physical conditions within molecular clouds is important.

We thank B. Baud for assistance with the observations, Dr. M. M. Litvak for many helpful discussions, and Professor A. Dalgarno for useful suggestions concerning the preparation of this manuscript. Radio astronomy at Harvard is supported by NSF grant MPS-74-24063.

REFERENCES

Aannestad, P. A. 1973, *Ap. J. Suppl.*, **25**, 233 (No. 217).
Barnard, E. E. 1927, *Photographic Atlas of Selected Regions of the Milky Way*, ed. E. B. Frost, M. R. Calvert (Washington: Carnegie Institute of Washington).
Davis, J., and Vanden Bout, P. 1973, *Ap. Letters*, **15**, 43.
De Jong, T., Chu, S. I., and Dalgarno, A. 1975, *Ap. J.*, **199**, 69.
Duncan, J. 1920, *Ap. J.*, **51**, 4.
Elliot, K. H., and Meaburn, J. 1974, *Astr. and Ap.*, **34**, 473.
Goldreich, P., and Kwan, J. 1974, *Ap. J.*, **189**, 441.
Gottlieb, C. A., Penfield, H., Ball, J. A., Gottlieb, E. W., Litvak, M. M., and Lada, C. J. 1975, in preparation.
Herbig, G. H., and Rao, N. K. 1972, *Ap. J.*, **174**, 401.
Kahn, F. D. 1954, *B.A.N.*, **12**, 187 (No. 456).
———. 1969, *Physica*, **41**, 172.
Kaplan, S. A. 1966, *Interstellar Gas Dynamics* (New York: Pergamon).
Lada, C. J. 1975, Ph.D. dissertation, Harvard University.
Lada, C., Dickinson, D. F., and Penfield, H. 1974*a*, *Ap. J. (Letters)*, **189**, L35.
Lada, C. J., Gottlieb, C. A., Litvak, M. M., and Lilley, A. E. 1974*b*, *Ap. J.*, **194**, 609.
Lada, C. J., Gull, T. R., Gottlieb, C. A., and Gottlieb, E. W. 1976, *Ap. J.*, in press.
Loren, R. B., Peters, W. L., and Vanden Bout, P. 1975, *Ap. J.*, **195**, 75.
Osterbrock, D. E. 1957, *Ap. J.*, **125**, 622.

Penzias, A. A., Jefferts, K. B., and Wilson, R. W. 1971, *Ap. J.*, **165**, 229.
Pottasch, S. 1956, *B.A.N.*, **13**, 71 (No. 471).
———. 1958, *ibid.*, **14**, 29 (No. 482).
Spitzer, L., Jr. 1968, *Diffuse Matter in Space* (New York: Interscience).
Struve, O. 1937, *Ap. J.*, **85**, 208.
Thackeray, A. D. 1950, *M.N.R.A.S.*, **110**, 343.

CHARLES J. LADA: Center for Astrophysics, 60 Garden Street, Cambridge, MA 02138
JOHN H. BLACK: School of Physics and Astronomy, University of Minnesota, Minneapolis, MN 55455